International Journal of Nanomedicine

Dovepress

open access to scientific and medical research

Open Access Full Text Article

ORIGINAL RESEARCH

Selective Laser Efficiency of Green-Synthesized Silver Nanoparticles by *Aloe arborescens* and Its Wound Healing Activities in Normal Wounded and Diabetic Wounded Fibroblast Cells: In vitro Studies

This article was published in the following Dove Press journal:
International Journal of Nanomedicine

Sathish Sundar Dhilip Kumar
Nicolette Nadene Houreld
Heidi Abrahamse

Laser Research Centre, University of Johannesburg, Johannesburg, South Africa

Introduction: Silver nanoparticles (AgNPs) have been extensively used in wound healing applications owing to their valuable physicochemical and biological properties. The main objective of this study was to evaluate the combined effects of green-synthesized silver nanoparticles (G-AgNPs) and photobiomodulation (PBM; laser irradiation at 830 nm with 5 J/cm^2) in normal wounded and diabetic wounded fibroblast cells (WS1).

Methods: The combined effect of G-AgNPs and PBM was studied by various *in vitro* wound healing studies including cell morphology, cell migration rate and percentage wound closure, cell viability, cell proliferation, and filamentous (F)-actin and nuclear morphology staining.

Results: Cell viability results revealed good cellular compatibility of G-AgNPs to WS1 cells. The combined therapy of G-AgNPs and PBM demonstrated promising results to achieve progressive migration and wound closure in both normal wounded and diabetic wounded cell models. G-AgNPs alone and in combination with PBM had no negative effect on cell viability and proliferation, and there was an increase in cell migration.

Conclusion: Overall, these findings demonstrate that the combined treatment of G-AgNPs and PBM does not display any adverse effects on wound healing processes in both normal wounded and diabetic wounded cell models.

Keywords: green synthesis, silver nanoparticles, photobiomodulation, laser, wound healing, cell migration

Introduction

Infected wounds are a major health concern and burden to patients with diabetes, and in some cases these ulcers take more than 20 weeks to heal and frequently lead to amputation.[1] These ulcers are a major cause of disability and impact negatively on the patient's quality of life. The treatment and management of chronic diabetic wounds are often multidisciplinary.[2] Nowadays, silver-based dressings are actively used for the effective healing of infected diabetic wounds.[3] The application of nanoparticles (NPs) in the biological domain is an emergent field due to increasing levels of understanding of biological systems and their interaction with nanomaterials.[4] Silver nanoparticles (AgNPs) are

Correspondence: Sathish Sundar Dhilip Kumar
Laser Research Centre, Faculty of Health Sciences, University of Johannesburg, PO Box 17011, Doornfontein, Johannesburg 2028, South Africa
Fax +27 11 559 6884
Email sathishd@uj.ac.za

submit your manuscript | www.dovepress.com
DovePress
http://doi.org/10.2147/IJN.S257204

© 2020 Dhilip Kumar et al. This work is published and licensed by Dove Medical Press Limited. The full terms of this license are available at https://www.dovepress.com/terms.php and incorporate the Creative Commons Attribution – Non Commercial (unported, v3.0) License (http://creativecommons.org/licenses/by-nc/3.0/). By accessing the work you hereby accept the Terms. Non-commercial uses of the work are permitted without any further permission from Dove Medical Press Limited, provided the work is properly attributed. For permission for commercial use of this work, please see paragraphs 4.2 and 5 of our Terms (https://www.dovepress.com/terms.php).

known as metal-based nanomaterials and have been extensively used for different biological applications due to their physicochemical and biological properties.[5] AgNPs have potent antibacterial, antimicrobial and anti-inflammatory effects, which play a key role in promoting wound healing.[6,7] The use of AgNPs in the treatment of chronic wounds such as delayed chronic venous leg ulcers,[8,9] and post-burn residual wounds[10] is well documented.

Aloe arborescens (family Asphodelaceae) has been traditionally applied for its therapeutic and medicinal properties over thousands of years, including anti-inflammatory, antimicrobial, antibacterial, analgesic, anti-allergic, and antioxidant.[11–14] The non-toxic leaf sap extract (LSE) is a mucilage that can influence wound healing[13] and acts as a stabilizing, reducing and capping agent for NPs via the green synthesis method.[11,15] This method of preparation is suitable for large-scale synthesis and avoids the usage of synthetic or chemical-based agents. The green synthesis method possesses good tolerability and efficacy and is inexpensive as compared to current options.[16,17]

Photobiomodulation (PBM) has been shown to be effective in the treatment of normal and diabetic wounds by stimulating cellular processes. It involves the use of low powered light (typically light emitting diodes (LED) or lasers) to treat and heal a variety of conditions. It has been used with success and shown to influence extensive healing of different wounds.[18–20] Ayuk et al (2012) reported that laser irradiation of diabetic wounded human skin fibroblast cells resulted in increased cellular migration, viability, proliferation, and collagen production compared to non-irradiated cells.[21] It is well documented that PBM stimulates normal cellular processes in wound healing, and AgNPs have shown positive effects by reducing bacterial levels and promotes wound healing mechanisms. However, the combined effect of AgNPs and PBM is not well documented. Therefore, the primary objective of this study was to evaluate the combined effects of G-AgNPs and PBM (laser irradiation at 830 nm with 5 J/cm^2) in normal wounded and diabetic wounded fibroblast cells (WS1). We used the central scratch assay to stimulate a wound in WS1 human skin fibroblast cells. The central scratch assay has been widely used to create a wound or gap in the confluent monolayer of cells to mimic a wound *in vitro*.[22,23] A wavelength of 830 nm and a fluence of 5 J/cm^2 was chosen as these parameters have been previously shown to stimulate WS1 cells and induce positive effects on diabetic wounded fibroblast cells.[24] It has also been reported that a similar wavelength and fluence increases cutaneous wound tensile strength in a diabetic murine model.[25]

Materials and Methods

Cell Culture (2D)

WS1 human skin fibroblast cells were used for experiments. All cell line experimental procedures performed in this study was approved by the Faculty of Health Sciences Research Ethics Committee of the University of Johannesburg (REC-01-27-2017). All methods and procedures were performed in accordance with the relevant guidelines and regulations. All chemicals and reagents used in the study were of analytical grade. Deionized water (MilliQ element, 18 Mohm/cm) was used for all the experiments. Human skin fibroblast cells (WS1, ATCC®, CRL-1502™) were grown in minimum essential medium (MEM, M7278, Sigma–Aldrich, South Africa) supplemented with 10% (v/v) fetal bovine serum (FBS, F9665, Sigma–Aldrich, South Africa), 2 mM L-glutamine solution (G7513, Sigma–Aldrich, South Africa), 100 U Penicillin and 100 µg/mL Streptomycin (P4333, Sigma–Aldrich, South Africa), 2.5 µg/mL Amphotericin-B (A2942, Sigma–Aldrich, South Africa), 1 mM sodium pyruvate (S8636, Sigma– Aldrich, South Africa), and 0.1 mM non-essential amino acids (NEAA, M7145, Sigma–Aldrich, South Africa).

Two models, namely normal wounded (NW) and diabetic wounded (DW), and eight groups were used, namely non-irradiated normal wounded (NW 0J), non-irradiated G-AgNP treated normal wounded (NW 0J NP), irradiated normal wounded (NW 5J), irradiated G-AgNP treated normal wounded (NW 5J NP), non-irradiated diabetic wounded (DW 0J), non-irradiated G-AgNP treated diabetic wounded (DW 0J NP), irradiated diabetic wounded (DW 5J), and irradiated G-AgNP treated diabetic wounded (DW 5J NP). A diabetic model was achieved by continuously growing cells in MEM (basal glucose concentration of 5.6 mMol/L) containing an additional 17 mMol/L glucose.[23] To determine the effects of PBM cells were detached by adding TrypLE™ express (1 mL/25 cm^2, Gibco 12563–029, Life Technologies, South Africa) and incubated for 3 min at 37°C. For experiments, excluding proliferation studies, 6 x 10^5 cells were seeded into 3.4 cm diameter tissue culture plates as determined by the Trypan blue exclusion test, and plates were incubated overnight at

37°C in 5% CO_2 to allow cells to attach. For proliferation studies, 10^6 cells were seeded.

A wound was simulated whereby the cell monolayer was scratched down the center with a sterile disposable 1 mL pipette.[26] The selected groups were treated with 12 µg/mL G-AgNPs, incubated for 30 min and then irradiated. Untreated and non-irradiated (0 J/cm^2) cells served as controls. It was reported in our previous study that the selected concentration (12 µg/mL G-AgNPs) showed a satisfactory level of bactericidal activity against both Gram-positive and Gram-negative pathogenic bacterial cells[11] and hence, we used a concentration of 12 µg/mL in all assays.

Laser Irradiation

The laser was supplied by the Council of Scientific and Industrial Research (CSIR), National Laser Centre (NLC) of South Africa. In this study, a diode laser emitting at a wavelength of 830 nm was used. Laser parameters are summarized in Table 1. Cells were irradiated in 3.4 cm diameter tissue culture plates in 1 mL of culture medium in the dark, from above, with the culture dish lid off. Irradiation was performed at a distance of 7 cm, which created a spot size of 9.1 cm^2 that directly corresponded to the area of the tissue culture plate. After the desired time of incubation (24 and 48 h), cellular responses were evaluated by different methods.

Cell Viability

The Cell Titer-Glo® luminescent cell viability assay (Promega G7573, Anatech Analytical Technology, South Africa) is based on the quantification of intracellular adenosine triphosphate (ATP) which indicates the presence of metabolically active cells.[27] The assay measures the luminescent signal produced by the conversion of ATP to adenosine monophosphate (AMP) by the enzyme luciferase. Cells were treated with a range of concentrations of G-AgNPs (4, 8, and 16 µg/mL) and incubated for 48 h. Untreated cells were kept as controls. After treatment and incubation, equal volumes of reagent and cell suspension (50 µL) were added and mixed for 2 min to induce cell lysis. The plate was allowed to incubate at room temperature for 10 min to stabilize the luminescent signal. Luminescence was read in Relative Light Units (RLU) on a multilabel counter (Perkin Elmer, VICTOR3™, 1420).

Table 1 Laser Parameters

Light Source	Diode Laser
Wavelength (nm)	830
Emission	Continuous wave
Power output (mW)	104
Power density (mW/cm^2)	11.4547
Spot size (cm^2)	9.1
Fluence/energy density (J/cm^2)	5
Irradiation time	7 min 16 s

Cellular Morphology, Migration Rate and Percentage Wound Closure

Cellular morphology for all groups was captured using the live cell imaging microscope, Carl Zeiss Axio Observer Z1. Images were taken in the same spot at different time intervals (0, 24, and 48 h). The Axio vision LE (SE64 Rel. 3.9.1 SP1) software was utilized to measure wound closure (diameter in µm). Cell migration rate and percentage wound closure were calculated as per the procedure reported by Fox et al, 2017.[28]

The cell migration rate towards the center of the scratch was observed in normal wounded and diabetic wounded cells at 24 and 48 h. The migration rate was expressed in µm/h and calculated using the equation (A):

$$\text{Migration rate}(\mu\text{m/h}) = \left[\frac{(\text{Pre}-\text{migration})_{\text{length}} - (\text{Migration})_{\text{length}}}{\text{Time(h)}}\right] \quad \text{(A)}$$

where (pre-migration)$_{\text{length}}$ was the initial wound length (µm) at 0 h and (migration)$_{\text{length}}$ was the wound length at a particular time (h).

The percentage of wound closure was expressed in percentage and calculated using the equation (B):

$$\text{Wound closure}(\%) = \left[\frac{(\text{Pre}-\text{migration})_{\text{length}} - (\text{Migration})_{\text{length}}}{(\text{Pre}-\text{migration})_{\text{length}}}\right] \times 100 \quad \text{(B)}$$

where (pre-migration)$_{\text{length}}$ was the initial wound length (µm) at 0 h and (migration)$_{\text{length}}$ was the wound length at a particular time.

Cell Apoptosis

The assay uses Annexin V–fluorescein isothiocyanate (FITC) and propidium iodide (PI) (BD Biosciences, 556547, The Scientific Group, South Africa) to identify phosphatidyl serine sites on the membrane of apoptotic cells, as well as sites of membrane damage in necrotic cells, respectively. The assay was done according to the

manufacturer's instructions and analyzed on the BD Accuri™ C6 flow cytometer. Annexin V–FITC is detected as green fluorescence and PI as red. After treatment and incubation, the cells from all the groups were detached and washed with Hanks Balanced Salt Solution (H9394, Sigma-Aldrich, South Africa). Cells were resuspended in the 1X binding buffer at a concentration of 10^6 cells/mL, and 100 µL of the cell suspension was transferred into flow cytometry tubes. Five microliters each of the Annexin V–FITC and PI reagents were added and mixed and incubated for 10 min at room temperature in the dark. Flow cytometric analysis was performed within one hour at a rate of 400 events per second with a limit of 350 µL.

Cell Proliferation

The BD Pharmingen™ BrdU FITC Flow Kit (BD Biosciences, 559619/557891, The Scientific Group, South Africa) was used to measure cell proliferation. BrdU is included into newly synthesized DNA during the S-phase of the cell cycle. The assay was done according to the manufacturer's instructions and analysed on the BD Accuri™ C6. After treatment and desired incubation (24 and 48 h), 10^6 cells/mL were labeled with 10 µL of 1 mM BrdU and incubated for 1 h at 37°C. Cells were rinsed with 1 mL of staining buffer and the supernatant was discarded after centrifugation for 5 min at 300 g. The pellet was resuspended in BD Cytofix/Cytoperm™ buffer and incubated for 10 min on ice. Cells were rinsed and centrifuged as previously mentioned and the pellet resuspended in BD Cytoperm™ Permeabilization Buffer Plus and incubated for 10 min. Cells were washed and centrifuged as previously mentioned and the pellet was resuspended and incubated for 1 h at 37°C in 300 µg/mL DNase in Dulbecco's phosphate-buffered saline (DPBS). Cells were rinsed and resuspended in BD Perm/Wash™ Buffer containing anti-BrdU and incubated for 20 min at room temperature. Cells were washed and resuspended in 1 mL staining buffer and analyzed by flow cytometry at a rate of 400 events per second with a limit of 350 µL.

Filamentous Actin (F-Actin) and Nuclear Morphology Analysis

Filamentous actin and nuclear morphology were determined by staining with Rhodamine Phalloidin (RP) and Hoechst, respectively. Phalloidin is a seven amino acid peptide toxin from the mushroom *Amanita phalloides*, which binds specifically with the polymerized form of actin (F-actin) and is excited at 535–585 nm. Hoechst is a bis-benzimidazole derivative compound that binds to the minor groove of DNA and is often used for fixed- and live-cell fluorescent staining of DNA and nuclei in cellular imaging techniques. Hoechst is a cell-permeable DNA stain excited by UV light and emits blue fluorescence at 460–490 nm. After treatment and desired incubation (24 and 48 h), cells were incubated with 200 µL of 100 nM RP (# PHDR1, Cytoskeleton, Inc. Biocom Africa (Pty) Ltd, South Africa) for 30 min at 37°C in a humidified atmosphere in the dark. After three washes with PBS, nuclei were counterstained with 1 µg/mL Hoechst 33258 (861405, Sigma-Aldrich, South Africa) for 10 min at 37°C in a humidified atmosphere in the dark, and washed three times with PBS. A fluorescence microscope (Carl Zeiss, AXIO Observer Z1) was used to evaluate F-actin and nuclear morphology.

Statistical Analysis

All graphs were created with GraphPad Prism (Version 5.01). All experiments were done in triplicate to monitor for the reproducibility of the results, and data are expressed as the mean ± standard deviation. Statistical analysis was performed using SigmaPlot version 13.0. Differences between groups were determined using the one-tailed Student's *t*-test and One-Way Analysis of Variance (ANOVA). The differences were statistically significant when $P \leq 0.05$.

Results and Discussion

AgNPs are extensively studied for their multifunctional biological applications which include their non-toxic, biocompatible, antimicrobial and anti-inflammatory activities.[29] The anti-inflammatory properties of AgNPs play a major role in wound healing whereby it suppresses inflammatory events during the early phases of wound healing in both *in vivo* and *in vitro* models.[30,31] PBM-based therapies are non-invasive and stimulate cellular pathways in wound repair and regeneration.[32,33] In recent investigations, the combined therapy of metal-based nanoparticles with PBM has been studied in the treatment of wounds (*in vivo*). The synergistic effect of this combined therapy has shown antibacterial activity against pathogenic bacteria as well as the promotion of wound healing. Lau et al (2016) recently reported on the combined use of GNPs and PBM (808 nm diode laser with a total fluence of 5 J/cm^2) in an *in vivo* cutaneous wound model. The

histological results revealed that the combined treatment had an optimal effect on wound healing by promoting angiogenesis and collagen production.[34] In another study, Khan et al (2016) used gold nanorods and a Nd-YAG laser (1064 nm) and evaluated the potential of the combined therapy in a pathogen infected *in vivo* wound model. The treatment results revealed a reduced number in bacterial counts and accelerated wound healing.[35]

In our previous study, we reported that LSE extracted from *A. arborescence* has fundamental properties to act as a reducing, capping and stabilizing agent to produce G-AgNPs via the green synthesis approach, and G-AgNPs possessed excellent physicochemical and antibacterial properties. The synthesized G-AgNPs demonstrated a satisfactory level of bactericidal activity against human pathogenic bacteria (*Staphylococcus aureus* and *Pseudomonas aeruginosa*).[11] In view of these observations and in continuation of our previous work in wound healing, we tested the combined effects of G-AgNPs and PBM in normal wounded and diabetic wounded WS1 cell models through different methods, including cellular morphology, viability and proliferation, cellular migration rate and percentage wound closure, apoptosis, and F-actin and nuclear morphology studies.

Cellular Viability

In the present study, the biocompatibility of different concentrations of synthesized G-AgNPs (4, 8, and 16 µg/mL) was evaluated *in vitro* using the Cell Titer-Glo® luminescent cell viability assay (Figure 1). The different concentrations of G-AgNPs were compared to the control, and there was no significant difference at 4 µg/mL ($p = 0.437$), 8 µg/mL ($p = 0.446$) and 16 µg/mL ($p = 0.457$). The results showed that no prominent cell death occurred during treatment with G-AgNPs, and cellular viability of G-AgNP treated cells was comparable with that of the control. Thus, there was good cellular compatibility of G-AgNPs against WS1 cells. According to our previous report, 8 µg/mL and 12 µg/mL of G-AgNPs were required to achieve Minimum inhibitory concentration (MIC) in Gram-positive and Gram-negative bacterial cells, respectively[11] and hence, we used the maximum concentration of 12 µg/mL in the remainder of the assays. Galandakova et al (2015) evaluated cellular toxicity of AgNPs in fibroblast cells and reported that a concentration of up to 25 µg/mL is non-toxic and is the

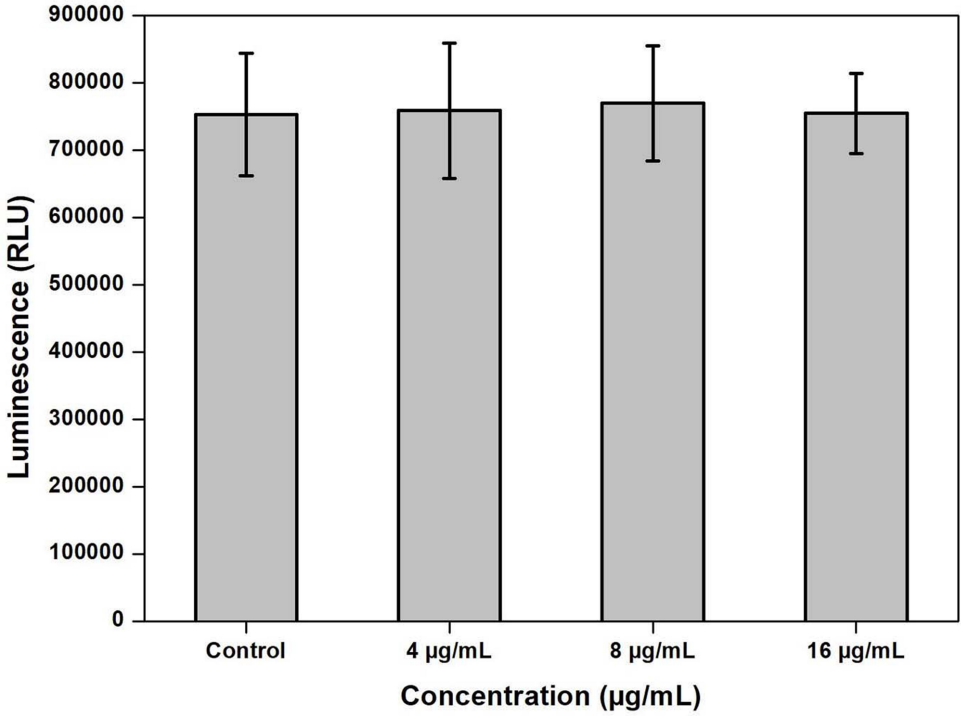

Figure 1 Cellular viability as assessed by the CellTiter-Glo® luminescent cell viability assay. Cellular viability was determined in WS1 cells treated with different concentrations of G-AgNPs (4, 8 and 16 µg/mL). Untreated cells were used as a control and analysed 48 h post-treatment.
Abbreviations: µg/mL, microgram per microliter; RLU, relative light units; G-AgNPs, green-synthesized silver nanoparticles.

most suitable candidate as a topical agent for wound healing applications.[36]

Cellular Morphology, Migration Rate, and Percentage Wound Closure

Cellular morphology, migration rate, and percentage wound closure were examined. The distance between the wound margins was measured at different time intervals (0, 24, and 48 h), and the corresponding time-lapse images for normal wounded and diabetic wounded cell models are given in Figures 2 and 3, respectively. We observed that the morphology of the WS1 cells appeared flat and spindle-shaped (bi or multipolar projections) in all the studied groups at 24 and 48 h in both normal wounded and diabetic wounded models, which concurs with recently reported findings.[21,37]

Cell migration is considered as an important step in wound healing, and it directly indicates how fast a treatment promotes complete wound closure.[28] The migration rate (μm/h) was obtained from the live cell imaging experiments for both normal wounded and diabetic wounded models and is depicted in Figures 4A and

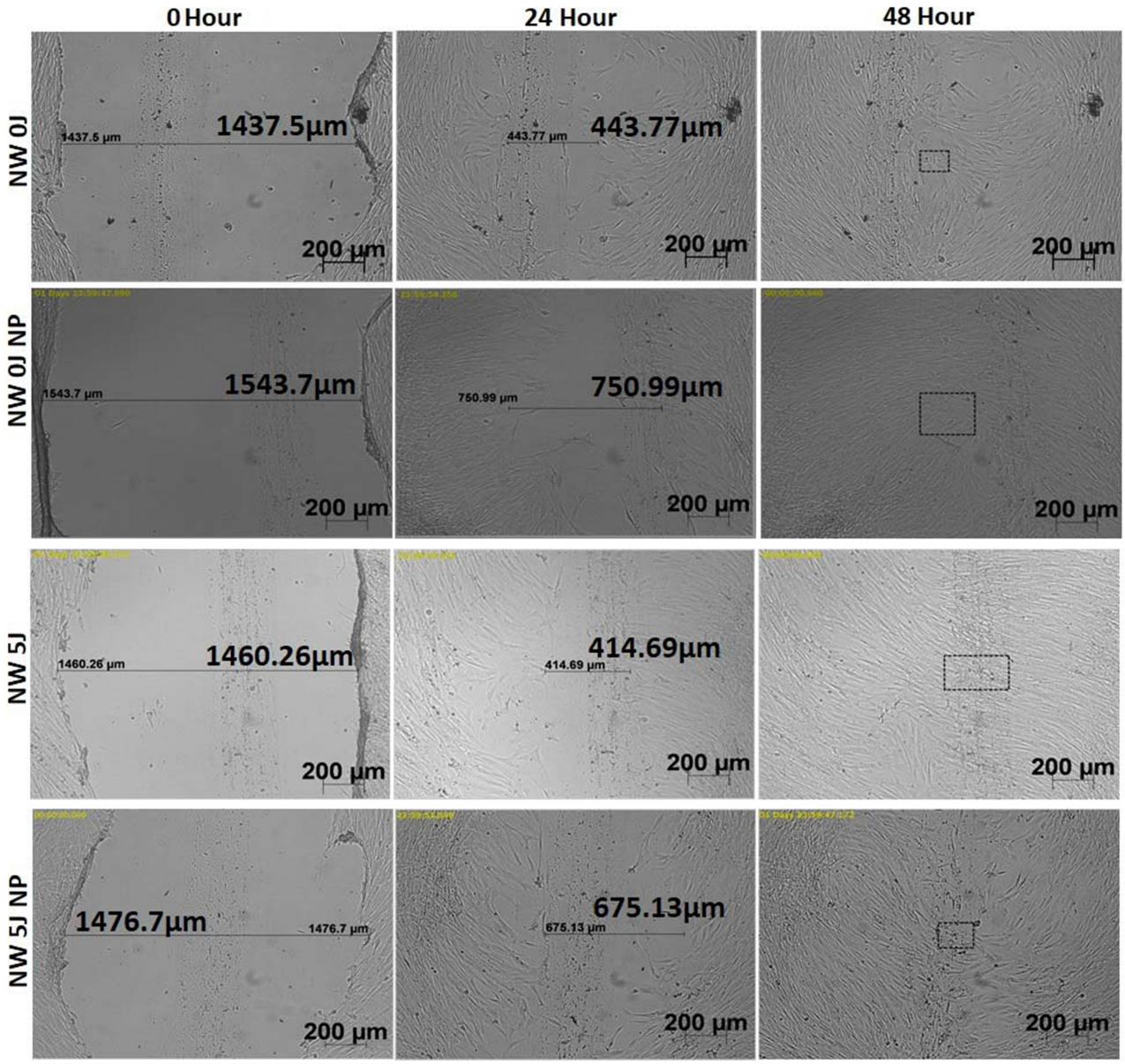

Figure 2 Time-lapse micrographs of non-irradiated normal wounded cells (NW 0J); non-irradiated, G-AgNP treated normal wounded cells (NW 0J NP); irradiated, normal wounded cells (NW 5J); and irradiated, G-AgNP treated normal wounded cells (NW 5J NP), analysed at 0, 24 and 48 h.
Abbreviations: μm, micrometer; G-AgNP, green-synthesized silver nanoparticle.

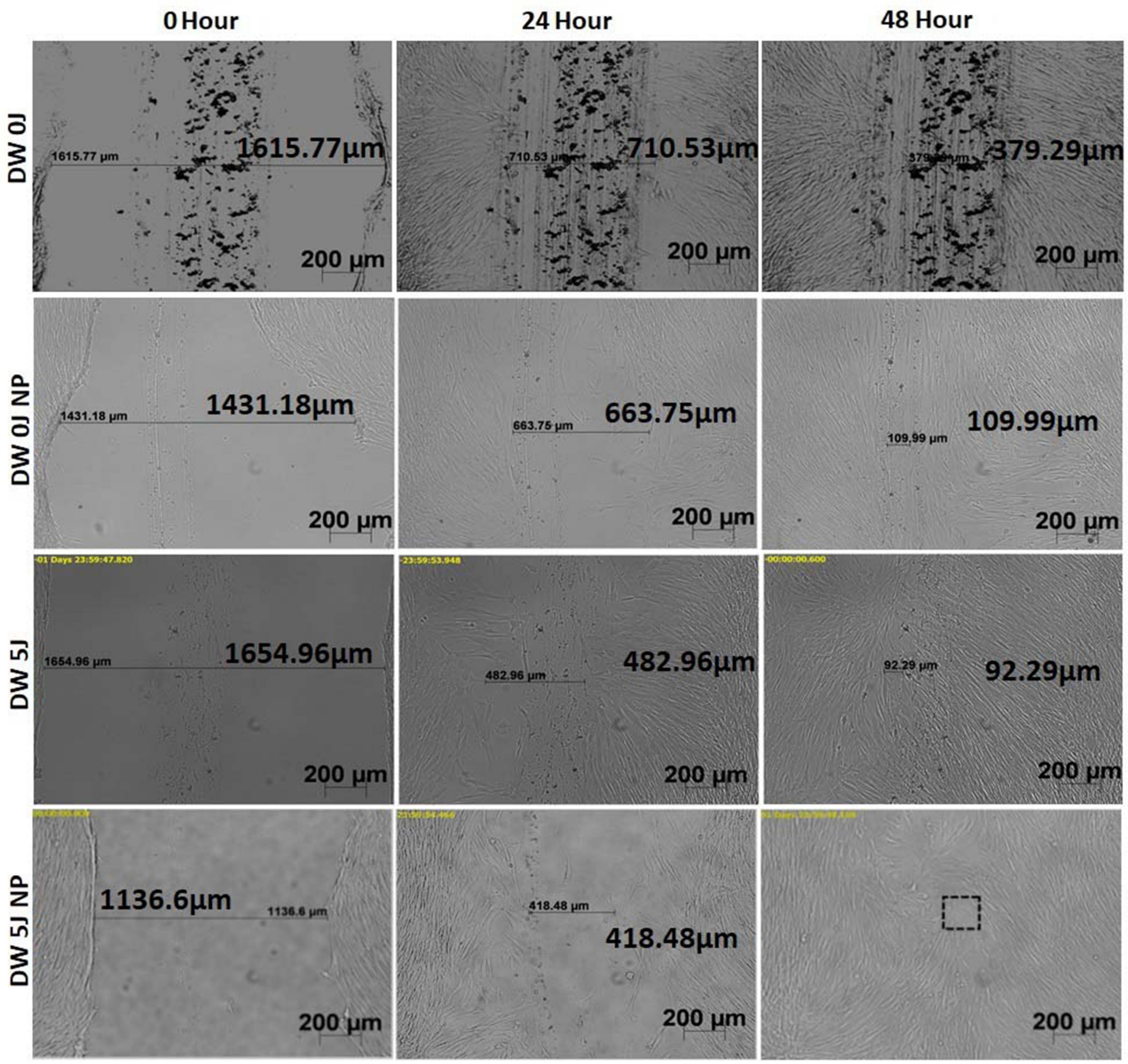

Figure 3 Time-lapse micrographs of non-irradiated diabetic wounded cells (DW 0J); non-irradiated, G-AgNP treated diabetic wounded cells (DW 0J NP); irradiated, diabetic wounded cells (DW 5J); and irradiated, G-AgNP treated diabetic wounded cells (DW 5J NP), analysed at 0, 24 and 48 h.
Abbreviations: µm, micrometer; G-AgNP, green-synthesized silver nanoparticle.

5A, respectively. In the normal wounded model at 24 h (Figure 4A), both non-irradiated G-AgNP treated normal wounded cells ($p < 0.05$) and irradiated G-AgNP treated normal wounded cells ($p < 0.01$) showed a significant decrease in migration rate compared to baseline, non-irradiated normal wounded cells (NW 0J). A significant increase was observed in irradiated normal wounded cells compared to irradiated G-AgNP treated normal wounded cells ($p < 0.01$). At 48 h there was complete wound closure thus no measurements could be taken.

In the diabetic wounded model at 24 h (Figure 5A), migration rate was significantly increased in irradiated diabetic wounded cells compared to the non-irradiated diabetic wounded cells ($p < 0.01$), and irradiated G-AgNP treated diabetic wounded cells ($p < 0.01$). Migration rate was significantly decreased in non-irradiated G-AgNP treated diabetic wounded cells ($p < 0.01$) and irradiated G-AgNP treated diabetic wounded cells ($p < 0.05$) compared to the non-irradiated diabetic wounded cells. There was no statistically significant difference between irradiated G-AgNP treated diabetic

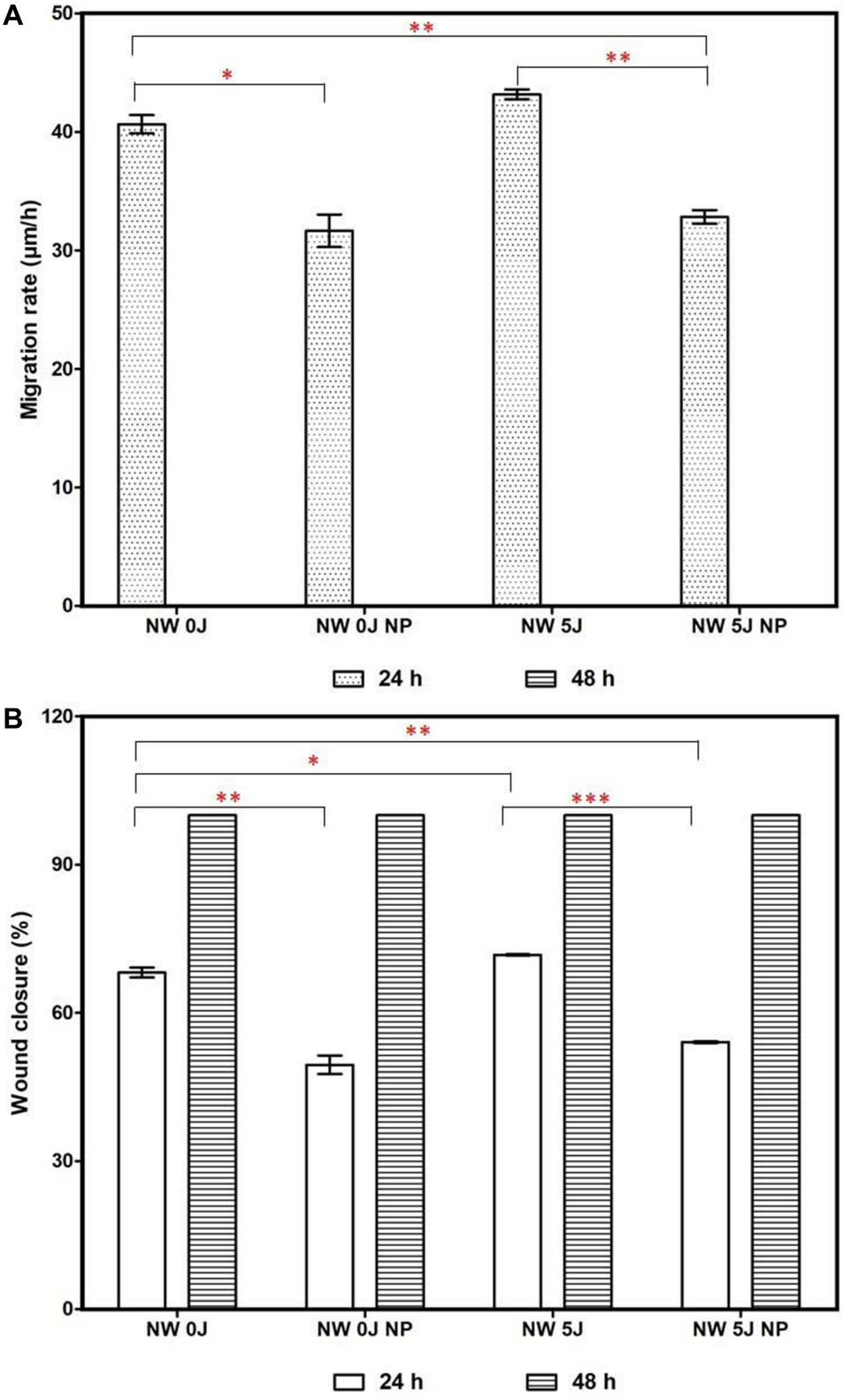

Figure 4 Migration rate (µm/h = micrometer per hour) – (**A**) Non-irradiated normal wounded (NW 0J); non-irradiated, G-AgNP treated normal wounded (NW 0J NP); irradiated normal wounded (NW 5J); and irradiated, G-AgNP treated normal wounded (NW 5J NP) WS1 cells were analysed at 24 and 48 h (hours). (**B**) Wound closure (%) - Non-irradiated normal wounded (NW 0J); non-irradiated, G-AgNP treated normal wounded (NW 0J NP); irradiated normal wounded (NW 5J); and irradiated, G-AgNP treated normal wounded (NW 5J NP) WS1 cells were analysed at 24 and 48 h. Significance is shown as *p<0.05, **p<0.01 and ***p<0.001. G-AgNP = Green-synthesized silver nanoparticle.

Abbreviation: G-AgNP, green-synthesized silver nanoparticle.

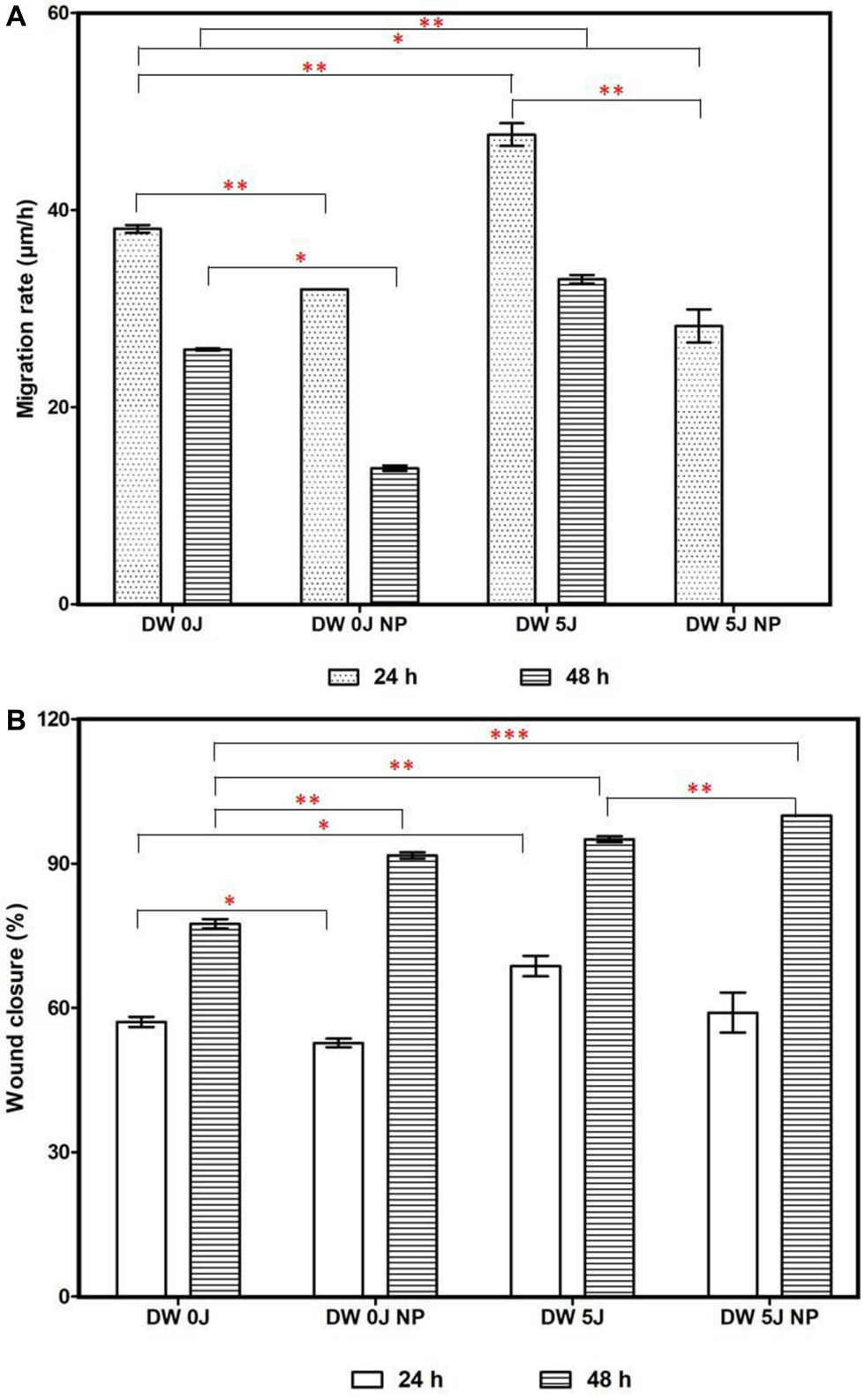

Figure 5 Migration rate (µm/h = micrometer per hour) – (**A**) Non-irradiated diabetic wounded (DW 0J); non-irradiated, G-AgNP treated diabetic wounded (DW 0J NP); irradiated diabetic wounded (DW 5J); and irradiated, G-AgNP treated diabetic wounded (DW 5J NP) WS1 cells were analysed at 24 and 48 h (hours). (**B**) Wound Closure (%) - Non-irradiated diabetic wounded (DW 0J); non-irradiated, G-AgNP treated diabetic wounded (DW 0J NP); irradiated diabetic wounded (DW 5J); irradiated G-AgNP treated diabetic wounded (DW 5J NP) WS1 cells analysed at 24 and 48 h. Significance is shown as *p<0.05, **p<0.01 and ***p<0.001.
Abbreviations: G-AgNP, green-synthesized silver nanoparticle.

wounded cells and non-irradiated G-AgNP treated diabetic wounded cells ($p = 0.079$). At 48 h, the migration rate was significantly increased in irradiated diabetic wounded cells ($p < 0.01$) and decreased in non-irradiated G-AgNP treated diabetic wounded cells ($p < 0.05$) compared to the non-irradiated diabetic wounded cells.

The percentage of wound closure was obtained from the live cell imaging experiments for both normal wounded and diabetic wounded models and is depicted in Figures 4B and 5B, respectively. In the normal wounded model at 24 h (Figure 4B), wound closure (%) was significantly increased in irradiated normal wounded cells compared to irradiated G-AgNP treated normal wounded cells ($p < 0.001$) and non-irradiated normal wounded cells ($p < 0.05$). Wound closure was significantly decreased in non-irradiated G-AgNP treated normal wounded cells ($p < 0.01$) and irradiated G-AgNP treated normal wounded cells ($p < 0.01$) compared to non-irradiated normal wounded cells. There was no statistically significant difference between irradiated G-AgNP treated normal wounded cells and non-irradiated G-AgNP treated normal wounded cells ($p = 0.068$). At 48 h, all normal wounded groups showed complete wound closure.

In the diabetic wounded model at 24 h, there was a significant increase in percentage wound closure (Figure 5B) in irradiated diabetic wounded cells compared to non-irradiated diabetic wounded cells ($p < 0.05$), while no significant difference between irradiated G-AgNP treated diabetic wounded cells and non-irradiated G-AgNP treated diabetic wounded cells ($p = 0.140$) was observed. There was a significant decrease in percentage wound closure in non-irradiated G-AgNP treated diabetic wounded cells compared to non-irradiated diabetic wounded cells. No significant differences were observed between irradiated diabetic wounded cells and irradiated G-AgNP treated diabetic wounded cells ($p = 0.087$). Complete wound closure was achieved over 48 h in irradiated G-AgNP treated diabetic wounded cells (100%), while only 77% wound closure was achieved in non-irradiated diabetic wounded cells, 91% in non-irradiated G-AgNP treated diabetic wounded cells and 95% in irradiated diabetic wounded cells. At 48 h, wound closure (%) was significantly increased in non-irradiated G-AgNP treated diabetic wounded cells ($p < 0.01$), irradiated diabetic wounded cells ($p < 0.01$), and irradiated G-AgNP treated diabetic wounded cells ($p < 0.001$) compared to non-irradiated diabetic wounded cells.

A comparison between normal wounded and diabetic wounded cell models was performed at 24 h for both cellular migration and wound closure studies. In the migration study, the results showed that there was a significant increase in normal wounded cells compared to diabetic wounded cells (non-irradiated $p = 0.006$; non-irradiated G-AgNP treated $p = 0.006$; irradiated $p = 0.007$; and irradiated G-AgNP treated $p = 0.025$). In the wound closure study, the results displayed a significant increase in percentage wound closure in non-irradiated normal wounded cells compared to non-irradiated diabetic wounded cells ($p = 0.017$). No statistically significant differences were observed in normal wounded cells compared to diabetic wounded cells (non-irradiated G-AgNP $p = 0.259$; irradiated $p = 0.291$; and irradiated G-AgNP treated $p = 0.359$).

Overall, we found a progressive migration rate and percentage wound closure in both normal wounded and diabetic wounded cell models. At 48 h, all groups in the normal wounded cell model showed complete wound closure. Therefore, there was no measurable wound length at 48 h. In the diabetic wounded model, we achieved complete wound closure at 48 h with the group treated with a combination of laser irradiation and G-AgNP treatment. It is well documented that laser irradiation at 830 nm has positive effects on diabetic wound healing[24] and earlier studies have confirmed that tannic acid-modified AgNP treatment can increase cell migration in HaCaT (immortalized human keratinocyte line) cells *in vitro*.[38] Thus, this study found that the addition of G-AgNPs at a concentration of 12 μg/mL with laser irradiation (at 830 nm with a fluence of 5 J/cm^2) showed no toxicity response to the cells and the migration rate and wound closure was very similar to their baseline (NW 0J and DW 0J) in both normal wounded and diabetic wounded cell models, with a beneficial effect on diabetic wounded cells.

Cell Apoptosis

The percentage of different cell population types (viable, early apoptosis (EA), late apoptosis (LA) and dead) were studied at 24 and 48 h using the FITC Annexin V/PI apoptosis assay by flow cytometry. The percentage of different stages of cells from both normal wounded and diabetic wounded models are shown in the supplementary information (see Supplementary Figure S1 and Figure S2). The percentage of viable cell counts from normal wounded and diabetic wounded models are shown in Figure 6A and 6B, respectively.

In normal wounded models (Figure 6A), the baseline (NW 0J) results were compared to all other groups and it

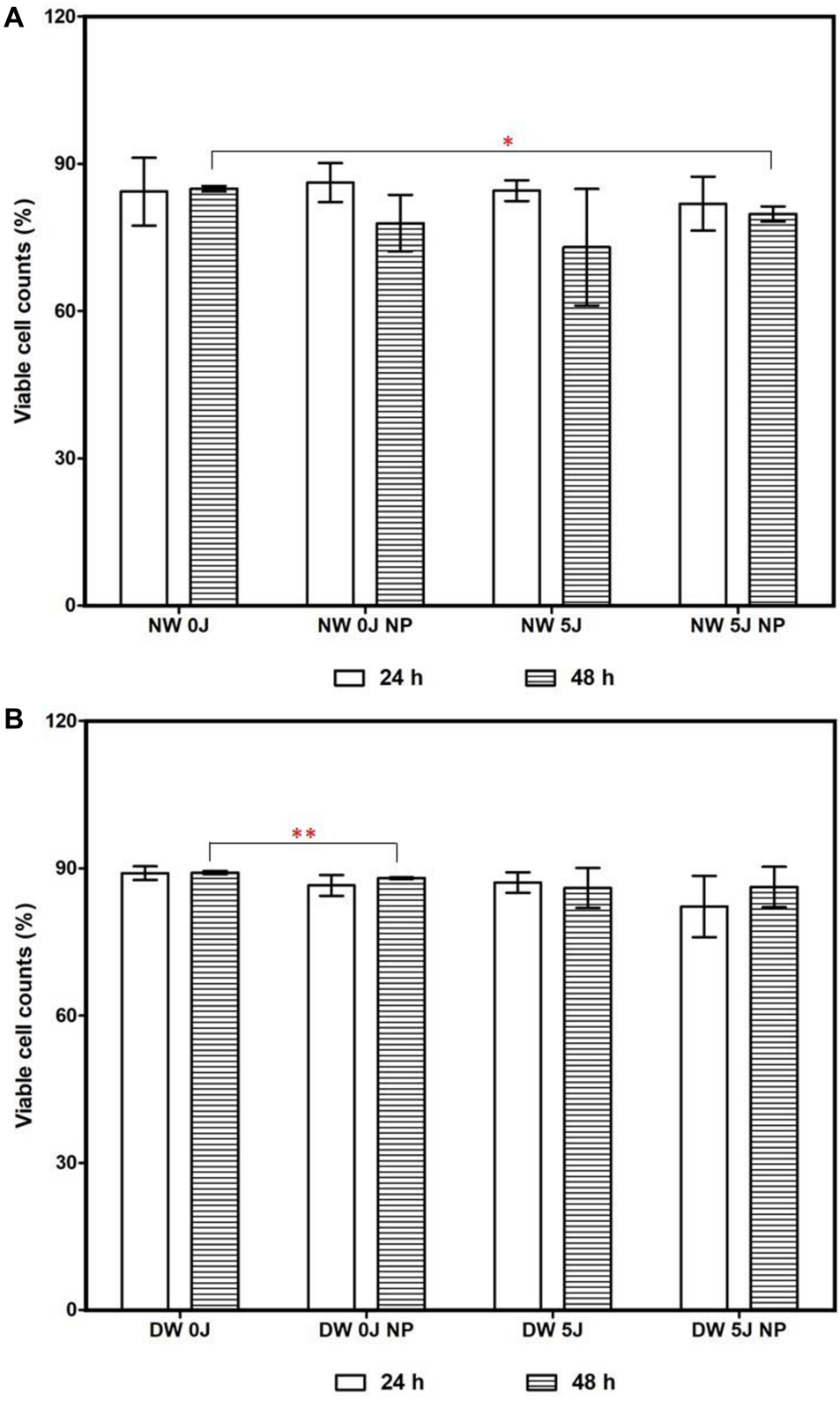

Figure 6 Determination of viable cell counts (%) measured by flow cytometry. (**A**) Non-irradiated normal wounded (NW 0J); non-irradiated G-AgNP treated normal wounded (NW 0J NP); irradiated normal wounded (NW 5J); and irradiated G-AgNP treated normal wounded (NW 5J NP) WS1 cells were analysed at 24 and 48 h (hours). Significance is shown as *p<0.05. (**B**) Non-irradiated diabetic wounded (DW 0J); non-irradiated G-AgNP treated diabetic wounded (DW 0J NP); irradiated diabetic wounded (DW 5J); and irradiated G-AgNP treated diabetic wounded (DW 5J NP) WS1 cells were analysed at 24 and 48 h. Significance is shown as *p<0.05 and **p<0.01.
Abbreviations: G-AgNP, green-synthesized silver nanoparticle.

showed that there was no significant differences at both 24 and 48 h, except for a significant decrease in irradiated G-AgNP treated normal wounded cells at 48 h ($p < 0.05$). In diabetic wounded models (Figure 6B), the baseline (DW 0J) results were compared to all other groups and it showed that there was no significant differences at both 24 and 48 h, except for a significant decrease in non-irradiated G-AgNP treated diabetic wounded cells (DW 0J NP) at 48 h ($p < 0.01$). In this context, we observed that cells reached a higher density at 48 h, which could promote contact inhibition of proliferation (CIP), a process that ceases all cell proliferation and cell division upon reaching confluence.[39]

A comparison between normal wounded and diabetic wounded cell models was performed at 24 and 48 h. At 24 h, results showed that there were no significant differences between normal wounded and diabetic wounded cell models (non-irradiated $p = 0.398$; irradiated $p = 0.289$; non-irradiated G-AgNP treated $p = 0.916$ and irradiated G-AgNP treated $p = 0.960$). At 48 h, a significant increase was observed in non-irradiated diabetic wounded cells ($p < 0.001$) compared to normal wounded cells; while there was no significant differences between irradiated ($p = 0.219$); non-irradiated G-AgNP treated ($p = 0.069$) and irradiated G-AgNP treated ($p = 0.108$). Thus, through this study, we observed that the combination of G-AgNPs treatment and PBM showed no adverse effect on cellular viability in both normal and diabetic wounded cell models at 24 and 48 h.

Cell Proliferation

Cell proliferation was examined by BrdU incorporation. The percentage of S-phase cell population values were plotted for normal wounded and diabetic wounded cell models and are shown in Figure 7A and 7B, respectively.

In normal wounded models (Figure 7A), the baseline (NW 0J) results were compared to all other groups and it showed that there was no significant differences at both 24 and 48 h in the percentage of S-phase cell populations, except for a significant increase in irradiated G-AgNP treated normal wounded cells at 24 h ($p < 0.05$). No significant differences seen were at 24 and 48 h in diabetic wounded models (Figure 7B). A comparison between normal wounded and diabetic wounded cell models was performed at 24 and 48 h for percentage of S-phase cell populations. At 24 h, results showed that there were no significant differences between normal wounded and diabetic wounded cell models (non-irradiated $p = 0.405$; irradiated $p = 0.107$; non-irradiated G-AgNP treated $p = 0.037$; and irradiated G-AgNP treated $p = 0.034$). Similarly, at 48 h, there was no significant differences (non-irradiated $p = 0.295$; irradiated $p = 0.385$, non-irradiated G-AgNP treated $p = 0.978$; and irradiated G-AgNP treated $p = 0.257$).

These results demonstrate that the combined treatment using G-AgNPs and PBM does not alter the cell proliferation mechanisms in S-phase during *in vitro* wound healing processes in both normal wounded and diabetic wounded cell models, which is supported by results seen in cell migration rate, percentage wound closure and viable cell counts. It is reported that the cell repair process predominantly involves both cell migration and cell proliferation in wound healing.[40] As we discussed earlier in the cell apoptosis study, a similar phenomenon, such as CIP, is involved for 48 h and may stop cell proliferation and cell division once cultures reach confluence.[39]

Filamentous Actin and Nuclear Morphology Analysis

F-actin and nuclear morphology in normal wounded (Figure 8A) and diabetic wounded cells (Figure 8B) was determined at 24 and 48 h using fluorescence microscopy. Hoechst (blue) stained cells showed no changes in nuclear shape, and the accumulation of Hoechst ensures its stiffness in all the groups studied in both normal wounded and diabetic wounded cell models. Rhodamine-Phalloidin (red) stained cells showed the presence of dense F-actin stress fibres in WS1 cells. The thickness and density of F-actin fibres were substantially increased at 48 h compared to 24 h in both normal wounded and diabetic wounded cell models, which may have occurred due to the reorganization of cytoskeletal F-actin fibres. In summary, these results demonstrate that G-AgNP and PBM did not cause any adverse effect on the normal structure of F-actin and nuclear morphology during the *in vitro* wound healing process. In wound healing, restoration or rearrangement of the cytoskeleton is considered an important process, and the dynamic changes of F-actin expression in the cytoskeleton are strongly associated with cell motility and wound repair mechanisms.[41,42]

Conclusion

We used a concentration of 12 µg/mL of G-AgNPs throughout this study and it revealed good cellular compatibility against WS1 cells. We found that G-AgNPs alone and in combination with PBM does not exhibit any adverse effects on cellular viability counts and does not

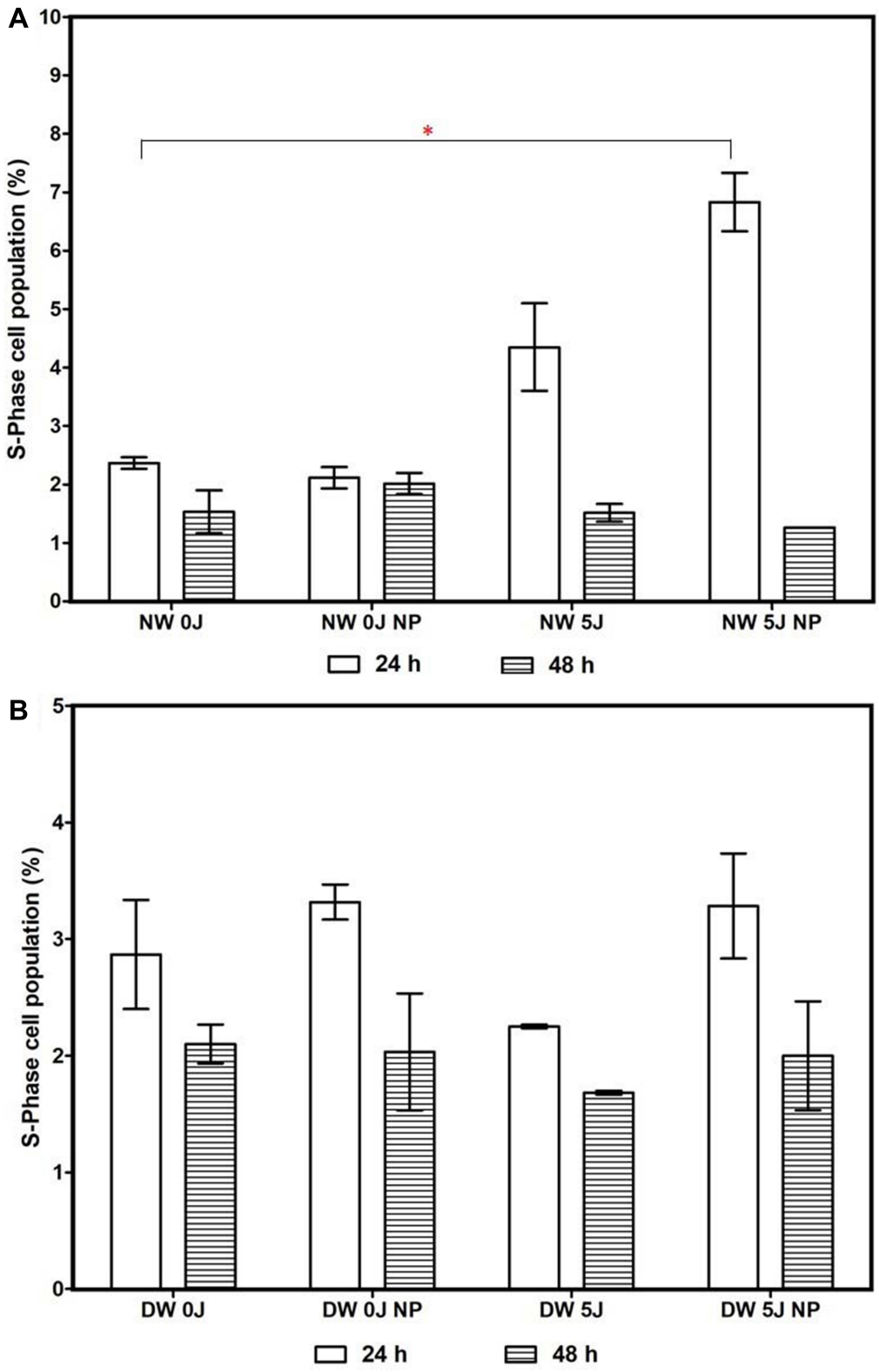

Figure 7 Determination of cell proliferation by BrdU incorporation in newly synthesized DNA as measured by flow cytometry (% of cells in proliferative, S-phase). (**A**) Non-irradiated normal wounded (NW 0J), non-irradiated G-AgNP treated normal wounded (NW 0J NP); irradiated normal wounded (NW 5J); and irradiated G-AgNP treated normal wounded (NW 5J NP) WS1 cells were analysed at 24 and 48 h (hours). (**B**) Non-irradiated diabetic wounded (DW 0J); non-irradiated G-AgNP treated diabetic wounded (DW 0J NP); irradiated diabetic wounded (DW 5J); and irradiated G-AgNP treated diabetic wounded (DW 5J NP) WS1 cells were analysed at 24 and 48 h. Significance is shown as *p<0.05.

Abbreviations: G-AgNP, green-synthesized silver nanoparticle.

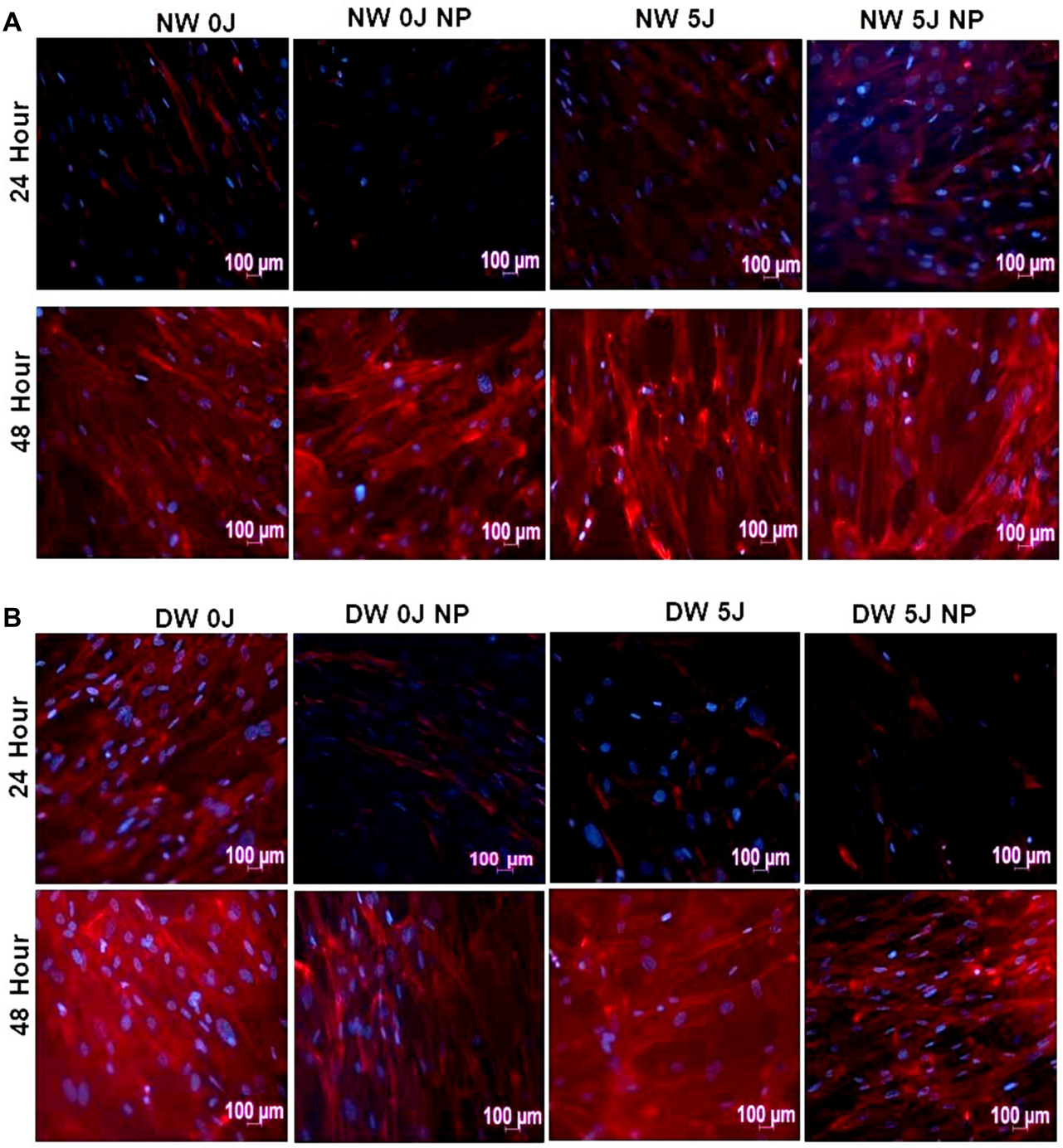

Figure 8 Filamentous actin (Rhodamine Phalloidin, red) and nuclear morphology (Hoechst stain, blue) analysis at 24 and 48 h. (**A**) Normal wounded (NW) cell models: non-irradiated (NW 0J); non-irradiated G-AgNP treated (NW 0J NP); irradiated (NW 5J); and irradiated G-AgNP treated (NW 5J NP). (**B**) Diabetic wounded (DW) cell models: non-irradiated (DW 0J); non-irradiated G-AgNP treated (DW 0J NP); irradiated (DW 5J); and irradiated G-AgNP treated (DW 5J NP).
Abbreviations: G-AgNP, green-synthesized silver nanoparticle.

alter the cell proliferation mechanisms in S-phase during *in vitro* wound healing processes in both normal wounded and diabetic wounded cell models. It exhibited a progressive migration rate, complete wound closure, and increased thickness and density of F-actin at 48 h. Overall, these findings suggest that the combination of G-AgNPs and PBM could be utilized in wound healing applications, including diabetic wound healing. However, *in vivo* trials on this combination therapy are required, as well as further pathogen infected *in vitro* models to unlock

the molecular mechanisms and their responses in wound healing.

Abbreviations

A. arborescens, *Aloe arborescens*; AgNPs, silver nanoparticles; AMP, adenosine monophosphate; ANOVA, analysis of variance; ATCC, American type culture collection; ATP, adenosine triphosphate; DNA, deoxyribonucleic acid; DW, diabetic wounded; DW 0J, diabetic wounded non-irradiated; DW 0J NP, G-AgNP treated diabetic wounded non-irradiated; DW 5J NP, G-AgNP treated diabetic wounded irradiated; DW 5J, diabetic wounded irradiated; FBS, foetal bovine serum; FITC, fluorescein isothiocyanate; G-AgNPs, green synthesized silver nanoparticles; GNPs, gold nanoparticles; LSE, leaf sap extract; MEM, minimum essential medium; MIC, minimum inhibitory concentration; NEAA, non-essential amino acids; Nd-YAG, neodymium-doped yttrium aluminum garnet laser; NIR, near-infrared laser; NPs, nanoparticles; NW 0J, normal wounded non-irradiated; NW 0J NP, G-AgNP treated normal wounded non-irradiated; NW 5J NP, G-AgNP treated normal wounded irradiated; NW 5J, normal wounded irradiated; NW, normal wounded; PBM, photobiomodulation; PBS, phosphate buffered saline; PI, propidium iodide; RLU, relative light units; RP, rhodamine phalloidin; UV, ultraviolet.

Acknowledgments

Sathish Sundar Dhilip Kumar is supported by funding from the Claude Leon Foundation, South Africa. This work is based on the research supported by the South African Research Chairs Initiative of the Department of Science and Technology and National Research Foundation of South Africa (Grant No 98337), as well as grants received from the University of Johannesburg (URC), the National Research Foundation (NRF), and the CSIR (Council for Scientific and industrial Research) – NLC (National Laser Centre) Laser Rental Pool Programme.

Author Contributions

SSDK conceptualized the idea and prepared the article. NNH was involved in drafting the manuscript, revising it critically for intellectual content, provided professional guidance and is the supervisor of lead author. HA organized this study and supplied editorial input. All authors read and approved the final manuscript. All authors contributed to data analysis, drafting, or revising the article, gave final approval of the version to be published, and agreed to be accountable for all aspects of the work.

Disclosure

The authors confirm that this article content has no conflict of interest

References

1. Katsilambros N, Dounis E, Makrilakis K, Tentolouris N, Tsapogas P. *Atlas of the Diabetic Foot*. 2nd ed ed. Oxford: Wiley-Blackwell; 2010.
2. Frykberg RG, Banks J. Management of diabetic foot ulcers: a review. *Fed Pract*. 2016;33:16–23.
3. El-Naggar MY, Gohar YM, Sorour MA, Waheeb MG. Hydrogel dressing with a nano-formula against methicillin-resistant staphylococcus aureus and pseudomonas aeruginosa diabetic foot bacteria. *J Microbiol Biotechnol*. 2016;26(2):408–420. doi:10.4014/jmb.1506.06048
4. Zhang XQ, Xu X, Bertrand N, et al. Interactions of nanomaterials and biological systems: implications to personalized nanomedicine. *Adv Drug Deliv Rev*. 2012;64:1363–1384. doi:10.1016/j.addr.2012.08.005
5. Dhilip Kumar SS, Rajendran NK, Houreld NN, Abrahamse H. Recent advances on silver nanoparticle and biopolymer-based biomaterials for wound healing applications. *Int J Biol Macromol*. 2018;115:165–175. doi:10.1016/j.ijbiomac.2018.04.003
6. Chaloupka K, Malam Y, Seifalian AM. Nanosilver as a new generation of nanoproduct in biomedical applications. *Trends Biotechnol*. 2010;28:580–588. doi:10.1016/j.tibtech.2010.07.006
7. Tian J, et al. Topical delivery of silver nanoparticles promotes wound healing. *Chem Med Chem*. 2006;2:129–136. doi:10.1002/cmdc.200600171
8. Rigo C, Ferroni L, Tocco I, et al. Active silver nanoparticles for wound healing. *Int J Mol Sci*. 2013;14:4817–4840. doi:10.3390/ijms14034817
9. Sibbald RG, Contreras-Ruiz J, Coutts P, et al. Bacteriology, inflammation, and healing: a study of nanocrystalline silver dressings in chronic venous leg ulcers. *Adv Skin Wound Care*. 2007;20:549–558. doi:10.1097/01.ASW.0000294757.05049.85
10. Huang Y, Li X, Liao Z, et al. A randomized comparative trial between Acticoat and SD-Ag in the treatment of residual burn wounds, including safety analysis. *Burns*. 2007;33:161–166. doi:10.1016/j.burns.2006.06.020
11. Dhilip Kumar SS, Houreld NN, Kroukamp EM, Abrahamse H. Cellular imaging and bactericidal mechanism of green-synthesized silver nanoparticles against human pathogenic bacteria. *J Photochem Photobiol B*. 2018;178:259–269. doi:10.1016/j.jphotobiol.2017.11.001
12. Mbanga J, Mangoma N, Saidi B. An Evaluation of the antimicrobial activities of A. barbadensis, A. chabaudii and A. arborescens leaf extracts used in folklore veterinary medicine in Zimbabwe. *J Anim Vet Adv*. 2010;9:2918–2923.
13. Jia Y, Zhao G, Jia J. Preliminary evaluation: the effects of Aloe ferox Miller and Aloe arborescens Miller on wound healing. *J Ethnopharmacol*. 2008;120:181–189. doi:10.1016/j.jep.2008.08.008
14. Amoo SO, Aremu AO, Van Staden J. In vitro plant regeneration, secondary metabolite production and antioxidant activity of micropropagated Aloe arborescens Mill. *Plant Cell Tissue Organ Cult*. 2012;111:345–358. doi:10.1007/s11240-012-0200-3
15. Altaf M, Jaganyi D. Characterization of triangular gold nanoparticles using Aloe arborescens leaf extract: a green synthesis approach. *Synth React Inorg Met-Org Nano-Metal Chem*. 2016;46:1332–1335. doi:10.1080/15533174.2015.1068810

16. Duan H, Wang D, Li Y. Green chemistry for nanoparticle synthesis. *Chem Soc Rev*. 2015;44:5778–57792. doi:10.1039/C4CS00363B
17. Makarov VV, Love AJ, Sinitsyna OV, et al. "Green" nanotechnologies: synthesis of metal nanoparticles using plants. *Acta Naturae*. 2014;6(1):35–44. doi:10.32607/20758251-2014-6-1-35-44
18. Houreld NN. Shedding light on a new treatment for diabetic wound healing: a review on phototherapy. *Sci World J*. 2014;2014:1–13. doi:10.1155/2014/398412
19. Kuffler DP. Photobiomodulation in promoting wound healing: a review. *Regen Med*. 2016;11:107–122. doi:10.2217/rme.15.82
20. Obradovic R. Low-level lasers as an adjunct in periodontal therapy in patients with Diabetes mellitus. *Diabetes Technol Ther*. 2012; 14:799–803. doi:10.1089/dia.2012.0027
21. Ayuk SM, Houreld NN, Abrahamse H. Collagen production in diabetic wounded fibroblasts in response to low intensity laser irradiation at 660 nm. *Diabetes Technol Ther*. 2012;14:1110–1117. doi:10.1089/dia.2012.0125
22. Jonkman JEM, Cathcart JA, Xu F, et al. An introduction to the wound healing assay using live-cell microscopy. *Cell Adh Migr*. 2014;8:440–451. doi:10.4161/cam.36224
23. Houreld N, Abrahamse H. Low-intensity laser irradiation stimulates wound healing in diabetic wounded fibroblast cells (WS1). *Diabetes Technol Ther*. 2010;12:971–978. doi:10.1089/dia.2010.0039
24. Houreld NN, Sekhejane PR, Abrahamse H. Irradiation at 830 nm stimulates nitric oxide production and inhibits pro-inflammatory cytokines in diabetic wounded fibroblast cells. *Laser Surg Med*. 2010;42:494–502. doi:10.1002/lsm.20812
25. Stadler I, Lanzafame RJ, Evans R, et al. 830-nm irradiation increases the wound tensile strength in a diabetic murine model. *Lasers Sur Med*. 2001;28:220–226. doi:10.1002/lsm.1042
26. Houreld N, Abrahamse H. Laser light influences cellular viability and proliferation in diabetic-wounded fibroblast cells in a dose- and wavelength-dependent manner. *Lasers Med Sci*. 2008;23:11–18. doi:10.1007/s10103-007-0445-y
27. Hawkins D, Abrahamse H. Laboratory methods for evaluating the effect of low level laser therapy (LLLT) in wound healing. *Afr J Biomed Res*. 2005;8:1–14.
28. Fox LT, Mazumder A, Dwivedi A, et al. In vitro wound healing and cytotoxic activity of the gel and whole-leaf materials from selected aloe species. *J Ethnopharmacol*. 2017;200:1–7. doi:10.1016/j.jep.2017.02.017
29. Zhang XF, Liu ZG, Shen W, Gurunathan S. Silver nanoparticles: synthesis, characterization, properties, applications and therapeutic approaches. *Int J Mol Sci*. 2016. doi:10.3390/ijms17091534.
30. Wright JB, Lam K, Buret AG, Olson ME, Burrell RE. Early healing events in a porcine model of contaminated wounds: effects of nanocrystalline silver on matrix metalloproteinases, cell apoptosis, and healing. *Wound Repair Regen*. 2002;10:141–151. doi:10.1046/j.1524-475X.2002.10308.x
31. Frankova J, Pivodova V, Vagnerova H, Juranova J, Ulrichova J. Effects of silver nanoparticles on primary cell cultures of fibroblasts and keratinocytes in a wound-healing model. *J Appl Biomater Func*. 2016;14:e137– e142.
32. Yadav A, Verma S, Keshri GK, Gupta A. Combination of medicinal honey and 904 nm superpulsed laser-mediated photobiomodulation promotes healing and impedes inflammation, pain in full-thickness burn. *J Photochem Photobiol B*. 2018;186:152–159. doi:10.1016/j.jphotobiol.2018.07.008
33. Ayuk SM, Abrahamse H, Houreld NN. The role of photobiomodulation on gene expression of cell adhesion molecules in diabetic wounded fibroblasts in vitro. *J Photochem Photobiol B*. 2016;161:368–374. doi:10.1016/j.jphotobiol.2016.05.027
34. Lau P, Bidin N, Islam S, et al. Influence of gold nanoparticles on wound healing treatment in rat model: photobiomodulation therapy. *Laser Surg Med*. 2016;49:380–386. doi:10.1002/lsm.22614
35. Khan MS, Bhaisare ML, Gopal J, Wu HF. Highly efficient gold nanorods assisted laser phototherapy for rapid treatment on mice wound infected by pathogenic bacteria. *J Ind Eng Chem*. 2016;36:49–58. doi:10.1016/j.jiec.2015.12.011
36. Galandakova A, Franková J, Ambrožová N, et al. Effects of silver nanoparticles on human dermal fibroblasts and epidermal keratinocytes. *Hum Exp Toxicol*. 2015;35:946–957. doi:10.1177/0960327115611969
37. Jere SW, Houreld NN, Abrahamse H. Photobiomodulation at 660 nm stimulates proliferation and migration of diabetic wounded cells via the expression of epidermal growth factor and the JAK/STAT pathway. *J Photochem Photobiol B*. 2018;179:74–83. doi:10.1016/j.jphotobiol.2017.12.026
38. Orlowski P, Zmigrodzka M, Tomaszewska E, et al. Tannic acid-modified silver nanoparticles for wound healing: the importance of size. *Int J Nanomed*. 2018;13:991–1007. doi:10.2147/IJN.S154797
39. Pavel M, et al. Contact inhibition controls cell survival and proliferation via YAP/TAZ-autophagy axis. *Nat Commun*. 2018:9. doi:10.1038/s41467-018-05388-x.
40. Zahm JM, Kaplan H, Hérard A-L, et al. Cell migration and proliferation during the in vitro wound repair of the respiratory epithelium. *Cell Motil Cytoskeleton*. 1997;37:33–43. doi:10.1002/(SICI)1097-0169(1997)37:1<33::AID-CM4>3.0.CO;2-I
41. Abreu-Blanco MT, Watts JJ, Verboon JM, Parkhurst SM. Cytoskeleton responses in wound repair. *Cell Mol Life Sci*. 2012;69:2469–2483. doi:10.1007/s00018-012-0928-2
42. Muller S, Djudjaj S, Lange J, et al. HIF stabilization inhibits renal epithelial cell migration and is associated with cytoskeletal alterations. *Sci Rep*. 2018;8. doi:10.1038/s41598-018-27918-9.

International Journal of Nanomedicine Dovepress

Publish your work in this journal

The International Journal of Nanomedicine is an international, peer-reviewed journal focusing on the application of nanotechnology in diagnostics, therapeutics, and drug delivery systems throughout the biomedical field. This journal is indexed on PubMed Central, MedLine, CAS, SciSearch®, Current Contents®/Clinical Medicine, Journal Citation Reports/Science Edition, EMBase, Scopus and the Elsevier Bibliographic databases. The manuscript management system is completely online and includes a very quick and fair peer-review system, which is all easy to use. Visit http://www.dovepress.com/testimonials.php to read real quotes from published authors.

Submit your manuscript here: https://www.dovepress.com/international-journal-of-nanomedicine-journal